References

1 THIAM, A., LEGROS, E., VUYE, S., ANDRÉ, P., WAWRZYNKOWSKI, E., and JOLY, C.: '40Gbit/s GaAs P-HEMT driver module for optical communications', *Electron. Lett.*, 1998, **34**, pp. 2232–2234

2 NOWOTNY, U., LAO, Z., THIEDE, A., LIENHART, H., HORNUNG, J., KAUFEL, G., KÖHLER, K., and GLORER, K.: '44Gbit/s 4:1 multiplexer and 50Gbit/s 2:1 multiplexer in pseudomorphic AlGaAs/GaAs-HEMT technology'. ISCAS '98, Monterey, California, USA, 1998

Temperature-insensitive UV-induced Bragg gratings in silica-based planar lightwave circuits on Si

Y. Hibino, M. Abe, T. Tanaka, A. Himeno, J. Albert, D.C. Johnson and K.O. Hill

A novel technique is proposed to realise temperature-insensitive Bragg gratings in silica-based lightwave circuits on Si using a bimetal plate. A wavelength shift < 0.15nm is successfully demonstrated between –40 and 80°C in the Bragg gratings written in a Mach-Zehnder interferometer.

Introduction: Bragg gratings can be formed in silica-on-silicon waveguides by irradiating them with UV lasers, such as those constructed in optical fibres. Planar-lightwave-circuit (PLC)-type devices such as filters [1, 2] and external cavity lasers [3] have been successfully demonstrated using UV-induced gratings. However, the Bragg wavelength in silica-on-silicon waveguides usually shifts with a temperature coefficient of ~0.01nm/°C because of the temperature dependence of the refractive index in silica glass. Temperature-insensitive gratings with stable characteristics are needed to allow the cost of the devices with UV gratings to be reduced and their field of application to be broadened. A polymer cladding technique has been described for fabricating a temperature-insensitive grating [4]. However, the refractive indices of polymers are usually sensitive to a humidity in an atmosphere because polymer materials absorb moisture.

Here, we propose a novel technique for realising temperature-insensitive Bragg gratings in silica-on-silicon waveguides using a bimetal plate attached to the bottom of an Si substrate with an adhesive. We successfully demonstrated a wavelength shift of < 0.15nm from –40 to 80°C in the Bragg gratings written in a Mach-Zehnder interferometer (MZI).

Calculation: Here, we consider a method of compensating the Bragg wavelength shift of an UV grating in a silica-on-silicon waveguide using a bimetal plate, assuming, for simplicity, that the stress is isotropic in the waveguide. A bimetal plate consists of two layers of metal with different thermal expansion coefficients. The warp δ of a bimetal plate changes with temperature as follows:

$$\delta = \frac{K(\Delta T/2)L^2}{4t_b} \qquad (1)$$

where K is the warping coefficient of the bimetal plate, ΔT is the temperature difference, and t_b and L are the thickness and length of the bimetal plate, respectively. If a bimetal plate is attached firmly to an Si substrate, the warp of the bimetal plate can be transferred to the substrate, and bending stress can be induced in the waveguide layer.

The Bragg wavelength λ_0 is given by the following equation

$$\lambda_0 = 2n_e\Lambda \qquad (2)$$

where n_e is the effective index of the waveguide and Λ is the grating pitch. The temperature dependence of the Bragg wavelength mainly results from that of n_e. Since the pitch is reduced by the stress applied to the waveguide, the Bragg wavelength shift caused by the temperature change can be compensated for by the warp of the bimetal plate attached to the Si substrate.

Experimental procedures: The sample configuration used in the experiment is shown in Fig. 1. It is an MZI with Bragg gratings written in both arms. The waveguides were fabricated on an Si substrate using the conventional PLC technologies of flame hydrolysis deposition and reactive ion etching. The refractive index difference between the core and the cladding was set at 0.3% and the core size at 8 × 8μm. The top and lower cladding thicknesses were ~30 and 20μm, respectively. The Si substrate was 1mm thick and the MZI chip was 25 × 4mm. The coupling ratio of the two couplers in the MZI was estimated to be ~45%. Two polarisation-maintaining (PANDA) fibres fixed in glass V-grooves were butted to one side facet of the chip using a conventional method to measure the temperature dependence of the gratings.

Bragg gratings 5mm in length were formed on the arms of the MZI by irradiating them with an ArF excimer laser through a phase mask [5]. The Bragg grating was written with an approximately 150mJ/cm²/pulse for 25minutes at an 100pps. This is described in more detail elsewhere [5].

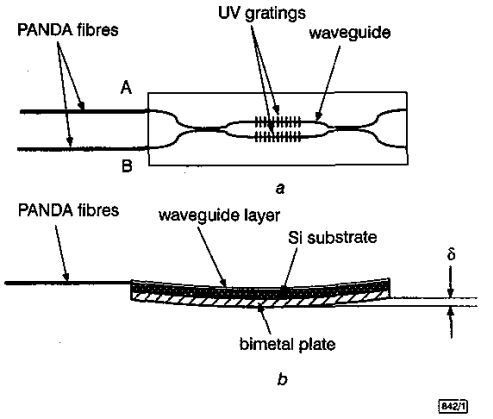

Fig. 1 *Schematic configuration of Mach-Zehnder interferometer with Bragg gratings on planar substrate to which a bimetal plate is attached*

a Top view
b Side view

We used a 1.5mm thick bimetal plate, of which the warp coefficient is ~1.5 × 10^{-5} (1/*K*), to compensate for the temperature dependence of the Bragg wavelength. The contracting side of the bimetal plate was attached to the bottom of the Si substrate using a thermally-curable epoxy adhesive as shown in Fig. 1. The size of the bimetal plate was set at 25 × 10mm.

To measure the temperature dependence of the Bragg wavelength, we placed the sample in a temperature-controlled chamber. The temperature of the sample in the chamber was monitored with a thermocouple. The spectra of the Bragg gratings from ports A to B in Fig. 1 were measured from –40 to 80°C using an amplified spontaneous emission (ASE) light source of an Er-doped amplifier and a spectrum analyser with a wavelength resolution of 0.007nm.

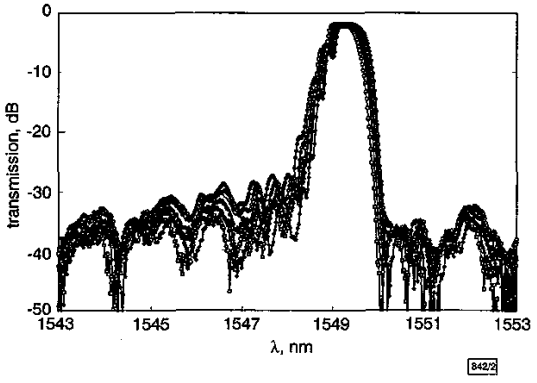

Fig. 2 *Transmission spectra of TE mode from ports A to B at different temperatures in sample with bimetal plate*

● –40°C
○ –20°C
—— 0°C
▲ 20°C
△ 40°C
□ 60°C
◇ 80°C

Results and discussion: The transverse electric (TE) mode spectra of the sample with the bimetal plate at different temperatures are shown in Fig. 2. It is noted that the Bragg grating peak does not shift significantly when the temperature is increased from –40 to 80°C. The bandwidth and crosstalk of the TE mode were also stable in this temperature range as shown in Fig. 2. Moreover, the spectra of the transverse magnetic (TM) mode were as stable as those of the TE mode at this temperature range.

The Bragg wavelengths of the sample with the bimetal plate for the TE and TM modes are plotted against temperature in Fig. 3. For comparison, the temperature dependences of the Bragg wavelength for a sample without a bimetal plate are shown by the lines in Fig. 3. We confirmed that the Bragg wavelength in silica-on-silicon waveguides without the bimetal plate shifted with a coefficient of ~0.011nm/°C for both the TE and TM modes. In contrast, it is clearly seen that the Bragg wavelengths of the TE and TM modes are stable and their changes are within 0.15nm even for a temperature range > 100°C.

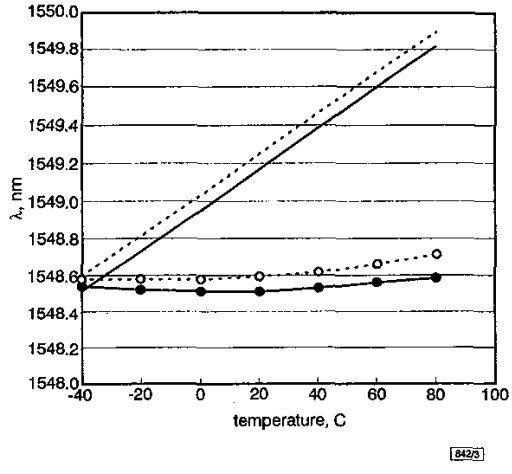

Fig. 3 *Bragg wavelengths of UV-written Bragg gratings against temperature*

● TE mode with bimetal plate
○ TM mode with bimetal plate
——— TE mode without bimetal plate
–·–·– TM mode without bimetal plate

The insertion losses of the sample are ~1.7dB around 25°C for both the TE and TM modes, including an excess loss caused by the offset of the coupling ratio of the directional couplers in the MZI, fibre-PLC chip coupling loss and connector loss. As shown in Fig. 2, the insertion losses are stable in the 0–80°C temperature range, and increase by ~0.5 dB at –40°C. We believe this loss increase is due to the deviation of the PANDA fibres butt-coupled to the chip at low temperature during the measurement.

The thickness of the bimetal plate needed to compensate for the temperature dependence of the Bragg wavelength was approximately half of the calculated value. This indicates that the warp of the bimetal plate may not have been transferred exactly to the Si substrate because the adhesive we used was not strong enough. However, the above results show that it is possible to form temperature-insensitive Bragg gratings in silica-on-silicon waveguides using a bimetal plate with an appropriate thickness.

Conclusions: We have successfully realised temperature-insensitive Bragg gratings in silica-based PLCs by attaching a bimetal plate to an Si substrate. We obtained a wavelength shift < 0.15nm in the Bragg gratings written in an MZI between –40 and 80°C. The conventional fabrication process, including the waveguide fabrication and fibre attachment processes, are unchanged in this technique. It is therefore possible to make a low-cost PLC-type device with temperature-insensitive Bragg gratings using the bimetal-plate technique.

Acknowledgments: We thank T. Miya for his encouragement.

17 August 1999
Electronics Letters Online No: 19991269
DOI: 10.1049/el:19991269

Y. Hibino, M. Abe, T. Tanaka and A. Himeno (*NTT Photonics Laboratories, Tokai, Ibaraki, 319-1193, Japan*)

J. Albert, D.C. Johnson and K.O. Hill (*Communication Research Centre, PO Box 11490, Station H, Ottawa,Ontario K2H 8SA, Canada*)

References

1 KASHYAP, R., MAXWELL, G.D. , and AINSLIE, B.J.: 'Laser-trimmed four-port bandpass filter fabricated in single-mode photosensitive Ge-doped planar waveguide', *IEEE Photonics Technol. Lett.*, 1993, **5**, pp. 191–194

2 HIBINO, Y., KITAGAWA, T., HILL, K.O., BILODEAU, F., MALO, B., ALBERT, J., and JOHNSON, D.C.: 'Wavelength division multiplexer with photoinduced Bragg gratings fabricated in a planar-lightwave-circuit-type asymmetric Mach-Zehnder interferometer on Si', *IEEE Photonics Technol. Lett.*, 1996, **8**, pp. 84–86

3 TANAKA, T., HIMENO, A., TAKAHASHI, H., KANEKO, A., HASHIMOTO, T., ABE, M., YAMADA, Y., INOUE, Y., and TOHMORI, Y.: 'Hybrid integrated external cavity laser without temperature-dependent mode hopping', *Electron. Lett.*, 1999, **35**, pp. 149–150

4 BOSC, D., LOISEL, B., MOISAN, M., DEVOLDERE, N., LEGALL, F., and ROLLAND, A.: 'Temperature and polarisation-insensitive Bragg gratings realised on silica waveguide on silicon', *Electron. Lett.*, 1997, **33**, pp. 134–136

5 ALBERT, J., BILODEAU, F., JOHNSON, D.C., HILL, K.O., MIHAILOV, S.J., STRYCKMAN, D., KITAGAWA, T., and HIBINO, Y.: 'Polarisation-independent strong Bragg gratings in planar lightwave circuits', *Electron. Lett.*, 1998, **34**, pp. 485–486

3.9W CW power from sub-monolayer quantum dot diode laser

A.E. Zhukov, A.R. Kovsh, S.S. Mikhrin, N.A. Maleev, V.M. Ustinov, D.A. Livshits, I.S. Tarasov, D.A. Bedarev, M.V. Maximov, A.F. Tsatsul'nikov, I.P. Soshnikov, P.S. Kop'ev, Zh.I. Alferov, N.N. Ledentsov and D. Bimberg

Diode lasers emitting at 947nm with sub-monolayer deposited InAs/GaAs quantum dots in the active region have been fabricated. The 3.9W output power limited by catastrophic optical damage and the peak conversion efficiency of 50.5% were achieved at 10°C in 100μm wide stripes with uncoated facets.

Introduction: 0.94–0.93μm high-power diode lasers are of great interest because of their applications as pump sources for yttrium aluminium garnet (YAG) solid-state lasers or Er-doped fibre amplifiers. A very high continuous-wave (CW) power of 10W has been achieved for 0.97μm InGaAs quantum well (QW) diode lasers [1, 2]. Quantum dot (QD) lasers have also demonstrated promising power characteristics. 3.5W CW power from 100μm wide *uncoated* apertures has been reported for a diode laser with InAs QDs formed in the Stranski-Krastanow (SK) growth mode [3]. The SK QDs in a GaAs matrix usually emit beyond the 1μm range. This use of an AlGaAs matrix is necessary to match the desirable 0.94–0.98μm wavelengths. However, this decreases the optical confinement factor. The deposition of a short-period InAs/(Al)GaAs superlattice on a GaAs(100) surface with an InAs effective thickness of less than 1 monolayer (ML) results in the formation of nanometre-scale (In,Ga)As QDs of a non-SK class [4 – 6]. The emission wavelength of QDs of this kind can be tuned over a relatively wide range (at least, 0.92–1μm) by varying the effective bias coverage, the thickness of GaAs spacers, and the number of repeatedly deposited pairs of InAs/GaAs. In this Letter we report the high-power operation of a 947nm QD diode laser with the active region formed by sub-monolayer (SML) deposition.

Experiment: The epitaxial structure was grown by solid-source molecular beam epitaxy on an n^+-doped GaAs(100) substrate. It consists of an n-type 0.3μm thick GaAs buffer, 1.2μm thick n- (p-) type (5×10^{17}cm^{-3}) $Al_{0.8}Ga_{0.2}As$ cladding layers surrounding an undoped graded-index waveguide, and a p^+-doped 0.6μm thick